Physical and Electrical Characterization of Mg-Doped ZnO Thin-Film Transistors

A. Shaw[a], T. J .Whittles[c], I. Z. Mitrovic[a], J. D. Jin[a], J. S. Wrench[b], D. Hesp[c], V. R. Dhanak[c], P. R. Chalker[b] and S. Hall[a]

[a]Department of Electrical Engineering and Electronics, University of Liverpool, Liverpool, UK.
[b]Centre for Materials and Structures, School of Engineering, University of Liverpool, Liverpool, UK.
[c]Stephenson Institute for Renewable Energy, University of Liverpool, Liverpool, UK.

Abstract—The effect of Mg-doping on the valence and conduction bands of ZnO grown at 200 °C using atomic layer deposition has been investigated using a range of physical characterization techniques: X-ray photoemission spectroscopy, inverse photoemission spectroscopy and spectrocopic ellipsometry. The conduction band minimum is seen to increase with Mg content hence confirming the increased band gap. The physical characterization has been linked with modeling of thin-film transistor structures whereby a defect state based model has been employed to explain the transport mechanisms within the film

Keywords— Zinc Oxide (ZnO), Mg doped ZnO (MgZnO), thin-film transistors (TFTs), Modeling, X-ray photoemission spectroscopy (XPS), inverse photoemission spectroscopy (IPES), Ellipsometry

I. INTRODUCTION

Zinc Oxide (ZnO) has seen a resurgence of interest in recent years due to its attractive properties for the transparent electronics industry namely from its large direct band gap (E_g) ~3.3 eV and exciton binding energy ~60 meV [1]. The current leading ZnO alloy is indium-gallium-zinc-oxide (IGZO) which has emerged as a leading alternative to a-Si:H in active matrix displays, allowing for higher refresh rates due to mobilities > 1 cm/Vs [2]. However, indium is a rare element and is known to suffer from large price fluctuations, hence, limiting its potential to dominate the transparent conductive oxide (TCO) market. Alternative dopants for ZnO such as F [3], Li [4] Mo [5] and Mg [6-7] have been implemented to improve the electrical characteristics of the films.

We recently published work on doping ratios of Mg and ZnO using atomic layer deposition (ALD) [6] where the optimum thin-film transistor (TFT) performance obtained was achieved with a cycle ratio of 7:1. X-ray diffraction indicated that the film crystallinity remained constant whilst varying the Mg content. However, as the Mg content was increased beyond cycle ratios higher than 7:1, there was a significant reduction in electron mobility presumably due to a large increase in impurity scattering. Furthermore, from photoluminescence spectra, E_g increased to 3.38 eV presumably due to the presence of MgO which has a bandgap E_g=7.8 eV [8].

The standard MOSFET equations are usually implemented in the literature to analyze conducting oxide TFT performance. However, in most cases, there is no distinct exponential and square law regime for the subthreshold and above threshold regions respectively. Such analysis therefore fails to explain the true transport mechanism within the ZnO channel. A defect state model based on multi-trapping and release [9] proposed by Torricelli et al. [10] is employed here. The model describes the current transport due to charge hopping between tail states near the conduction band. The defect traps are related to the disordered nature of the ZnO films.

In this paper we present further physical characterization of the Mg-doped ZnO (MgZnO) films using the photoelectron spectroscopic techniques (PES) of X-ray photoelectron spectroscopy (XPS) and inverse photoemission spectroscopy (IPES) to assess the effect of Mg content on the valence and conduction bands respectively. Moreover, the TFTs are analyzed with the defect state model using parameters derived from the physical characterization.

II. EXPERIMENTAL

The MgZnO films were deposited using ALD at 200 °C onto Si/SiO_2 substrates where the oxide thickness was 50 nm. The precursors used were H_2O, diethylzinc and bis(ethylcyclopentadienyl)magnesium, where doping was achieved by using the cycle ratio of 7:1 between the Zn and Mg precursors. For XPS and IPES measurements, two thicknesses, 5 nm and 20 nm, of the MgZnO were deposited for the interface and bulk measurements respectively. Samples of ZnO were also deposited onto the same Si/SiO_2 substrates with the same two thicknesses, to act as references. For the TFT fabrication, MgZnO films were deposited to a thickness of 50 nm. Using standard photolithography and lift-off processes, 80 nm of Al source and drain contacts were thermally evaporated and defined. The TFTs were isolated using acetic acid etchant. The Si substrate formed the back gate contact. Prior to electrical measurements, all the TFTs were annealed in air for 1 hour in order to reduce the conductivity of the films [11].

Photoelectron (PES) measurements for bulk and interfacial MgZnO/SiO_2 were performed in a standard ultra high vacuum chamber operating at a base pressure of less than $2x10^{-10}$ mbar with hydrogen as the main residual gas. Core level structure and the occupied density of states in the valence band was probed by XPS using a SPEXS monochromatic Al Kα X-ray source (hν = 1486.6 eV) operating at 200 W, and a PSP Vacuum Technology electron energy analyzer. The spectrometer was calibrated so that the Ag $3_{d5/2}$ photoelectron line had a binding energy (BE) of 368.27 eV, a full width at

half maximum (FWHM) of 0.6 eV being the spectral resolution for this study, and operating at a constant 10 eV pass energy. Charging of the samples was corrected by setting the C 1s peak (arising from adventitious carbon species) to 284.6 eV for all samples. The unoccupied density of states in the conduction band was measured by IPES using a PSP Vacuum Technology BaO cathode dispenser electron source and an isochromat NaCl photon detector, each mounted at an incidence angle of 45° to the sample normal. The IPES detector operates at a nominal resolution of 0.8 eV and the spectra were recorded over several hours to obtain good quality statistics. The energy scale was calibrated using the Fermi energy of a clean polycrystalline silver foil. Variable angle spectroscopic ellipsometry (VASE) measurements were performed using a spectral range from 0.5-5.5 eV, and angles of incidence of 65-75°, with 5° steps, to maximize the accuracy.

III. Results and Discussion

A. Physical Charaterization

The band gap of the ZnO and MgZnO films was estimated by linear extrapolation of the absorption coefficient curves in the non-absorbing regions, which was extracted from VASE experimental data. In Fig. 1 E_g is found to be 3.18 eV for ZnO and 3.37 eV for MgZnO. It is evident that Mg doping widens the band gap by about 0.2 eV.

The valence band offset (VBO) for the MgZnO/SiO_2 interface was determined by the Kraut method [12] using Si $2p_{3/2}$ and Zn $2p_{3/2}$ core levels (CLs) from the (50 nm) SiO_2 substrate, bulk (20 nm) MgZnO/SiO_2/Si and interfacial (5 nm) MgZnO/SiO_2/Si, using the formula

$$VBO = \delta_{SUB} + \delta_{INT} - \delta_{OXIDE} \quad (1)$$

where δ_{SUB}, and δ_{OXIDE} are the energy differences between the chosen reference core-levels in the substrate and bulk oxide samples and their respective valence band maxima (VBM), while δ_{INT} refers to the BE difference for the former two core-levels for the interfacial sample [12]. The error bar (± 0.15 eV) in estimating the valence band offset is due to valence band maximum (VBM) determination through the linear extrapolation method. The fitting of a Voigt function to the core-level peaks in order to determine the binding energies typically introduces a much smaller (± 0.05 eV) error. A Shirley-type background was used during the fitting of all spectra. The VBO for MgZnO/SiO_2 interface was found to be 1.9 ± 0.15 eV. This sees a change of 0.1 eV to the reference ZnO/SiO_2 film. This value is, however, within the error of determining the VBO by the Kraut method in this work, hence we can deduce no significant change in the position of the valence band edge for both the MgZnO/SiO_2 and ZnO/SiO_2 interfaces.

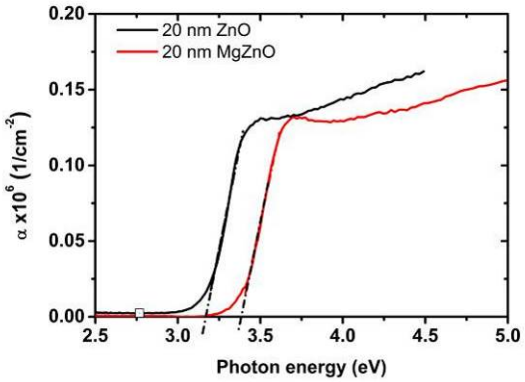

Fig. 1. Absorption coefficient vs photon energy for bulk 20 nm MgZnO and ZnO films on Si/SiO_2 extracted from VASE experimental data.

Linear extrapolation of the leading edges to the baselines of the XPS and IPES spectra at low binding energies for the bulk ZnO and MgZnO films yield the positions of the valence band maxima (E_{VBM}) and conduction band minima (E_{CBM}) respectively, referenced to the common Fermi level of the sample/spectrometer system. These band edge position values are shown in Fig. 2. The E_{VBM} positions for ZnO and MgZnO were found to be 2.29±0.05 eV and 2.37±0.05 eV respectively. These values show no significant change in the VBM position with the addition of Mg, as confirmed by the Kraut method. The E_{CBM} positions for ZnO and MgZnO were found to be 0.83±0.14 eV and 1.20±0.14 eV respectively. As the surface band gap can be extracted through the difference of the two determined band positions, one can confirm the band gap widening with the addition of Mg, demonstrated also in the VASE measurements shown in Fig. 1. The discrepancies between the size of the conduction band minima shift between the two techniques is noted and is believed to arise due to the surface sensitive nature of XPS/IPES which is measuring predominantly in the area where band bending will occur.

Flat band diagrams were constructed for the MgZnO on Si/SiO_2 by combining the Kraut method, XPS/IPES band edge determination and VASE results and are shown in Fig. 3 where it is assumed that the vacuum level is defined by the SiO_2 [13]. The discrepancy between the electron affinities (χ) are a result of the different band gaps obtained from the two measurement techniques.

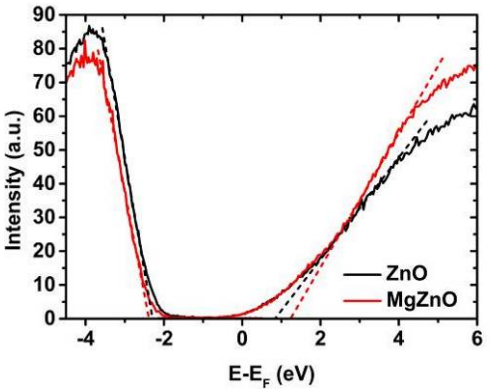

Fig. 2. Valence and conduction band edge obtained from XPS and IPES respectively for the ZnO and MgZnO films where the Fermi level is at 0 eV

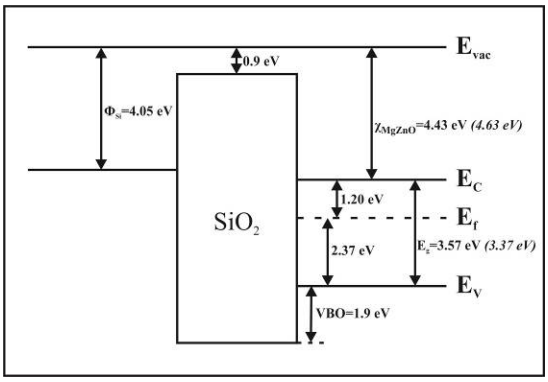

Fig. 3. Flat band diagrams for the $Si/SiO_2/MgZnO$ structures where the different E_g are derived from XPS and VASE *(italics)*

B. *Electrical Characterization*

The TFT output and transfer characteristics were measured using an Agilent B1500 parameter analyser and are shown in Figs. 4(a) and (b) respectively. The performance of the TFTs were benchmarked with the literature by comparing the effective saturation mobility (μ_{sat}) and threshold voltage (V_T) which were extracted assuming the standard MOSFET equation

$$I_{DS} = \frac{W}{2L}\mu_{sat} C_{ox}(V_{GS} - V_T)^2 \qquad (2)$$

where W and L are the channel width and length respectively, C_{ox} the gate oxide capacitance per unit area and V_{GS} the gate source voltage. The effective subthreshold swing (SS) was also extracted at the steepest part of the transfer slope using the following equation

$$SS = \left(\frac{d\log(I_{DS})}{dV_{GS}}\right)^{-1} \qquad (3)$$

Note that (3) also implies a standard Si model for the low current regime. This model is adopted at this stage, merely to allow comparison with values quoted in the literature. The on/off ratio ~$7x10^6$, where V_{on}= −0.6 V is the voltage required to establish a significant conducting channel [14]. Furthermore, μ_{sat}= 3.6 cm^2/Vs, V_T=8.1 V and SS= 0.8 V/dec.

However, it is apparent from the transfer characteristic in Fig. 4(a) that the subthreshold and above threshold regions do not follow an exponential and square law respectively but rather a generic power law over the entire on-region. Hence, we adopt the defect state model of Torricelli et al [10] with the following drain current expression

$$I_{DS} = \frac{W}{L}\beta\left[(V_{GS} - V_{FB} - \varphi_S)^\gamma - (V_{GS} - V_{FB} - \varphi_D)^\gamma\right] \qquad (4)$$

where V_{FB} is the flat band voltage, φ_S and φ_D the surface potentials at the source and drain, $\gamma = 2T_o/T$ where T is the temperature, T_o is the characteristic temperature associated with a single exponential trap distribution and β is defined as

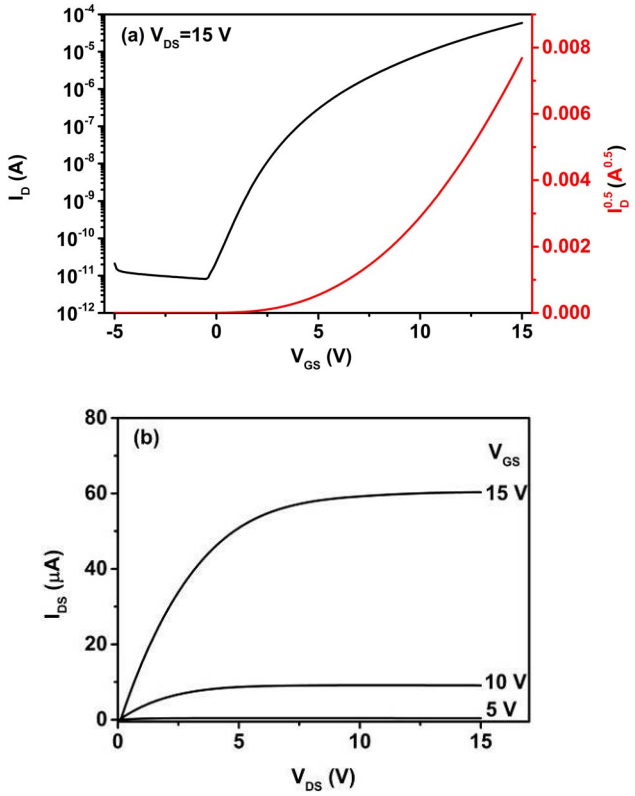

Fig. 4. (a) Transfer characteristic and $I_{DS}^{0.5}$-V_{GS} and (b) Output characteristic of the MgZnO TFT where W=400 μm, L=40 μm

$$\beta = \sigma_o \frac{\varepsilon_s}{C_{ox}} V_t \left(\frac{1}{\gamma - 1}\right)\left(\frac{C_{ox}^2 \sin\left(2\pi/\gamma\right)}{2\pi N_t q \varepsilon_s V_t}\right)^{\frac{\gamma}{2}} \qquad (5)$$

where σ_o is a conductivity pre-factor, ε_s is the permittivity of ZnO, N_t is the number of traps, q is the charge of an electron, and V_t is the thermal voltage (kT/q). The surface potentials φ_S are now defined as the source voltage and φ_D as the drain voltage in the triode region and V_{GS}-V_{FB} in the saturation region.

Using $V_{FB} = \phi_{Si} - \left(\chi_{MgZnO} + E_g/2 - \phi_f\right)$, the ideal V_{FB} was extracted from the band diagram in Fig. 3 where V_{FB}= −0.96 V and −1.03 V are obtained from the XPS/IPES and VASE results respectively. Using these ideal V_{FB} values (assuming no oxide charge), the device model parameters γ and β can be extracted graphically under the saturation condition writing (4) as $I_{DS} = W/L\,\beta(V_{GS} - V_{FB})^\gamma$ and taking logarithm the gradient gives γ and the intercept is (W/L)β.

Fig. 5 shows log (I_{DS}) against log (V_{GS}), using V_{FB} derived from the XPS/IPES and VASE results. For a V_{FB}= −0.96 V, γ=5.27 and β=$2.7x10^{-12}$ whereas when V_{FB}= −1.03 V, γ=5.32 and β=$2.3x10^{-12}$. The negative shift in V_{FB} causes an increase of the characteristic temperature from 791 to 798 K which implies an increase in disorder of the film. Using the extracted values for γ and β, the transfer and output characteristics were modeled using (4) and are given in Figs. 6(a) and (b) respectively. In Fig 6(a), for low V_{GS}, the fitting to the

measured data is poor which may arise from the change in gradient from in Fig. 5. However, the output characteristic in Fig 6(b) show an excellent fit across the entire range when V_{GS}= 5, 10 and 15 V, indicating that the model can be validated using the measured V_{FB} obtained from both XPS/IPES and VASE. The measured V_{FB} values enable a self-consistent fitting of the model with non-arbitrary parameters.

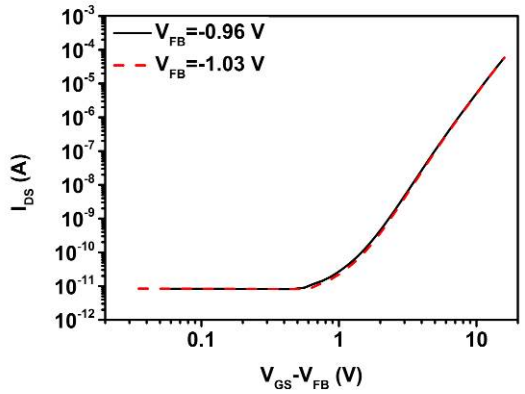

Fig. 5. log(I_{DS}) against log(V_{GS}-V_{FB}) for both V_{FB} from XPS/IPES (black) and VASE (red dash).

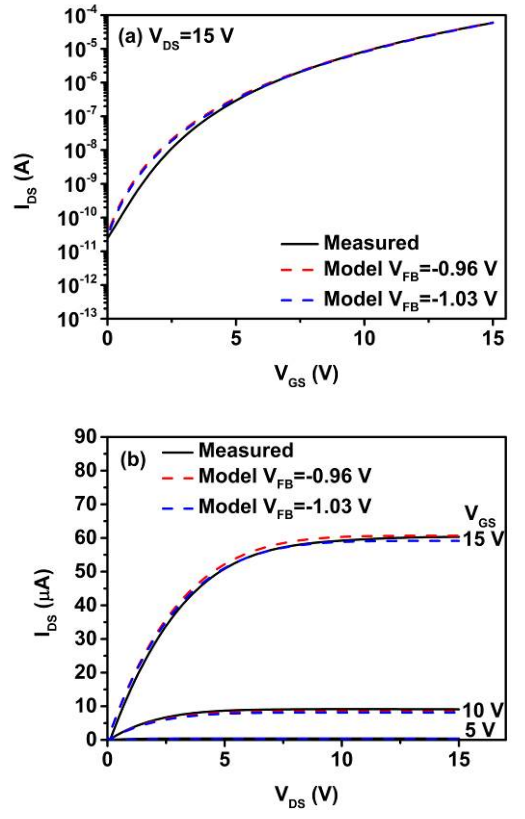

Fig. 6. (a) transfer and (b) output characteristics fitting using V_{FB} obtained from XPS/IPES (red dash) and VASE (blue dash)

IV. Conclusion

MgZnO TFTs have been accurately analysed using a defect state based model where the fitting parameter V_{FB} was extracted by three physical characterization techniques (XPS, IPES and VASE). The discrepancies between the flat band voltages can be explained by tolerances within the measurement techniques. We have confirmed and quantified that the band gap has increased with the incorporation of Mg where the VBO between ZnO and MgZnO remains constant, and consequently an energy shift occurs in the conduction band edge. Using both the V_{FB} values, self-consistent and realistic fitting parameters have been employed taking account of the disordered nature of the MgZnO films.

Acknowledgment

The authors acknowledge funding by the Engineering and Physical Science Research Council, UK, under project EP/K018884/1.

References

[1] U. Ozgur *et al*. "A comprehensive review of ZnO materials and devices", J. Appl. Phys., vol. 98, 2005.

[2] Y. Kuo, IEEE Proceedings of 2013 Twentieth international workshop on active matrix flat panel displays and devices (AM-FPD 13): TFT technologies and FPD materials, pp. 5–8, 2013.

[3] J. Chang *et al*., "Solution processed F doped ZnO (ZnO:F) for thin film transistors and improved stability through co-doping with alkali metals", J. Mater. Chem., vol 3, pp 1787, 2015.

[4] B. Y. Su, S. Y. Chu, Y. D. Juang, "Improved Electrical and Thermal Stability of Solution-Processed Li-Doped ZnO Thin-Film Transistors", IEEE T. Electron Devices. Vol. 59 (3), pp.700-704, 2012.

[5] L. Xu et al., "Tunable Electrical Properties in High-Valent Transition-Metal-Doped ZnO Thin-Film Transistors" IEEE Trans. Electron Devices, vol. 35(7), pp.759-761, 2014.

[6] J. S. Wrench *et al*., "Compositional tuning of atomic layer deposited MgZnO for thin film transistors". Appl. Phys. Lett. 105(20), pp. 202109. 2014.

[7] C. J. Ku *et al*., "Effects of Mg on the electrical characteristics and thermal stability of MgxZn1-xO thin film transistors". Appl. Phys. Lett. 98(12), pp 123511 – 123511, 2011.

[8] M. Wei, R. C. Boutwell, J. W. Mares, A. Scheurer, W. V. Schoenfeld, "Bandgap engineering of sol-gel synthesized amorphous $Zn_{1-x}Mg_xO$ films" Appl. Phys. Lett., vol. 98 (26), pp. 2619123, 2011.

[9] B. Movaghar, M. Grunewald, B. Pohlmann, D. Wurtz and W. Schirmacher, "Theory of hopping and multiple-trapping transport in disordered systems," J. Stat. Phys., vol. 30, pp. 315-334, 02/01, 1983.

[10] F. Torricelli et al., "Transport physics and device modeling of zinc oxide thin-film transistors part I: Long-channel devices," IEEE Trans. Electron Devices, vol. 58, pp. 2610-2619, 2011.

[11] J. D. Jin, Y. Luo, P. Bao, C. Brox-Nilsen, R. Potter, A. M. Song, "Tuning the electrical properties of ZnO thin-film transistors by thermal annealing in different gases", Thin Solid Films, vol . 552, pp. 192-195, (2014).

[12] E. A. Kraut, R. W. Grant, J. R. Waldrop, S. P. Kowalczyk, "Precise Determination of the Valence-Band Edge in X-Ray Photoemission Spectra: Application to Measurement of Semiconductor Interface Potentials". Phys. Rev. Lett., vol. 44, 1620–1623, 1980.

[13] J. Robertson, "Band offsets of wide-band-gap oxides and implications for future electronic devices", j. Vac. Sci. Technology B, vol. 18, pp. 1785-1791, 2000.

[14] R. L. Hoffman, C. Jagadish and S. Pearton, Eds., "Chapter 12 - ZnO thin-film transistors," Zinc Oxide Bulk, Thin Films and Nanostructures, Oxford: Elsevier Science Ltd, 2006, pp. 415-442.